Spin-torque microwave detector with out-of-plane precessing magnetic moment

O. V. Prokopenko*

Faculty of Radiophysics, Taras Shevchenko National University of Kyiv, Kyiv 01601, Ukraine

I. N. Krivorotov

Department of Physics and Astronomy, University of California, Irvine, CA 92697, USA

E. Bankowski and T. Meitzler

U.S. Army TARDEC, Warren, MI 48397, USA

S. Jaroch, V. S. Tiberkevich, and A. N. Slavin

Department of Physics, Oakland University, Rochester, MI 48309, USA

(Dated: January 18, 2012)

Operation of a spin-torque microwave detector (STMD) in a weak perpendicular bias magnetic field has been studied theoretically. It is shown that in this geometry a novel dynamical regime of STMD operation, characterized by large-angle out-of-plane magnetization precession, can be realized. The excitation of the large-angle precession has threshold character and is possible only for input microwave currents exceeding a certain frequency-dependent critical value. The output voltage of an STMD increases with the frequency of the input signal, but is virtually independent of its power. An STMD operating in the out-of-plane regime can be used as a non-resonant threshold detector of low frequency microwave signals and for applications in microwave energy harvesting.

I. INTRODUCTION

The spin-transfer torque (STT) carried by a spin-polarized electric current[1,2] can give rise to several types of magnetization dynamics (magnetization auto-oscillations and reversal) and, therefore, allows one to manipulate magnetization of a nano-scale magnetic object[3–7]. One of possible applications of the STT is the spin-torque microwave detector (STMD) based on the so-called spin-torque diode effect[8–11]. In an STMD, a microwave current $I_{\mathrm{RF}}(t) = I_{\mathrm{RF}} \sin(\omega t)$ is supplied to a magnetic tunnel junction (MTJ) structure and excites magnetization precession in the "free" magnetic layer (FL). The resistance oscillations $R(t)$ resulting from this precession mix with the driving current $I_{\mathrm{RF}}(t)$ to produce the output DC voltage $U_{\mathrm{DC}} = \langle I_{\mathrm{RF}}(t)R(t) \rangle$ (here $\langle \ldots \rangle$ denotes averaging over the period of oscillations $2\pi/\omega$ of the external microwave signal).

In the traditional regime of operation of an STMD[8–10] STT excites a *small-angle in-plane* (IP) magnetization precession about the equilibrium direction of magnetization in the FL of an MTJ (see the red dashed curve in Fig. 1). Below we shall refer to this regime of STMD operation as the IP-regime.

In contrast to the well-known IP-regime of STMD operation, in this paper we consider a *different regime of operation* of an STMD, based on the excitation of *large-angle out-of-plane* (OOP) magnetization precession under the action of an input microwave current $I_{\mathrm{RF}}(t)$ (see the blue dashed curve in Fig. 1). Using analytical and numerical calculations, we show that all the major

STMD characteristics in the OOP-regime qualitatively differ from the ones in the traditional IP-regime. In particular, excitations in the OOP-regime do not have a resonance character and exist in a wide range of driving frequencies. Also, the output DC voltage of an STMD in the OOP regime is almost independent of the input microwave power, provided it exceeds a certain threshold value. We believe that these properties of an STMD in the OOP-regime will be useful for the development of nano-sized threshold detectors with a large output DC voltage and also for the applications in microwave energy harvesting in the low-frequency region of the microwave band.

II. THEORY

A. Model

We consider a simple model of an STMD, formed by a circular MTJ nano-pillar (see Fig. 1). The magnetization of the pinned layer (PL) of the MTJ is assumed to be completely fixed and lie in the plane of the layer. The direction of the PL magnetization $\boldsymbol{p} = \hat{\boldsymbol{x}}$ determines the spin-polarization axis. The radius r of the MTJ nano-pillar is assumed to be sufficiently small, so that the magnetization of the free layer (FL) $\boldsymbol{M} \equiv \boldsymbol{M}(t)$ is spatially-uniform and can be treated in the macrospin approximation.

In contrast with the traditional IP-regime we assume that the STMD is biased by the *perpendicular* magnetic

Report Documentation Page

1. REPORT DATE **01 FEB 2012**	2. REPORT TYPE **Journal Article**	3. DATES COVERED **01-02-2012 to 01-02-2012**

4. TITLE AND SUBTITLE	5a. CONTRACT NUMBER
SPIN-TORQUE MICROWAVE DETECTOR WITH OUT-OF-PLANE PRECESSING MAGENETIC MOMENT	**W56HZV-11-P-A565**
	5b. GRANT NUMBER
	5c. PROGRAM ELEMENT NUMBER

6. AUTHOR(S)	5d. PROJECT NUMBER
Thomas Meitzler; Elena Bankowski; O. Prokopenko; A. Slavin; I. Krivorotov	5e. TASK NUMBER
	5f. WORK UNIT NUMBER

7. PERFORMING ORGANIZATION NAME(S) AND ADDRESS(ES)	8. PERFORMING ORGANIZATION REPORT NUMBER
Oakland University,Department of Physics,Rochester,MI,48309	**; #22528**

9. SPONSORING/MONITORING AGENCY NAME(S) AND ADDRESS(ES)	10. SPONSOR/MONITOR'S ACRONYM(S)
U.S. Army TARDEC, 6501 E.11 Mile Rd, Warren, MI, 48397-5000	**TARDEC**
	11. SPONSOR/MONITOR'S REPORT NUMBER(S) **#22528**

12. DISTRIBUTION/AVAILABILITY STATEMENT
Approved for public release; distribution unlimited

13. SUPPLEMENTARY NOTES
journal of applied physics journal article

14. ABSTRACT

Operation of a spin-torque microwave detector (STMD) in a weak perpendicular bias magnetic field has been studied theoretically. It is shown that in this geometry a novel dynamical regime of STMD operation, characterized by large-angle out-of-plane magnetization precession, can be realized. The excitation of the large-angle precession has threshold character and is possible only for input microwave currents exceeding a certain frequency-dependent critical value. The output voltage of an STMD increases with the frequency of the input signal, but is virtually independent of its power. An STMD operating in the out-of-plane regime can be used as a non-resonant threshold detector of low frequency microwave signals and for applications in microwave energy harvesting.

15. SUBJECT TERMS

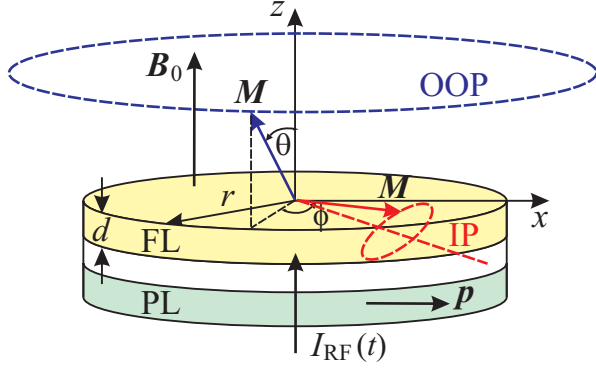| 16. SECURITY CLASSIFICATION OF:			17. LIMITATION OF ABSTRACT	18. NUMBER OF PAGES	19a. NAME OF RESPONSIBLE PERSON
a. REPORT **unclassified**	b. ABSTRACT **unclassified**	c. THIS PAGE **unclassified**	**Same as Report (SAR)**	**6**	

FIG. 1. Model of the considered system: circular nano-pillar of radius r consists of the "free" magnetic layer (FL) of thickness d and the "pinned" magnetic layer (PL). Under the action of microwave current $I_{\mathrm{RF}}(t) = I_{\mathrm{RF}} \sin(\omega t)$ magnetization vector $\boldsymbol{M}$ (shown by a blue arrow) is precessing along *large-angle out-of-plane* (OOP) trajectory (shown by blue dashed curve) about the direction of the bias magnetic field $\boldsymbol{B}_0 = \hat{\boldsymbol{z}} B_0$ ($B_0 < \mu_0 M_s$), μ_0 is the vacuum permeability, M_s is the saturation magnetization of the FL, $\boldsymbol{p} = \hat{\boldsymbol{x}}$ is the unit vector in the direction of the magnetization of the PL, $\hat{\boldsymbol{x}}$ and $\hat{\boldsymbol{z}}$ are the unit vectors of x- and z-axis, respectively. The red dashed curve is the trajectory of small-angle in-plane (IP) magnetization precession about equilibrium direction of magnetization in the FL (shown by a red dashed line), which exists in the traditional IP-regime of STMD operation.

field $\boldsymbol{B}_0 = \hat{\boldsymbol{z}} B_0$, which is *smaller* than the saturation magnetic field of the FL , i.e., $B_0 < \mu_0 M_s$ (μ_0 is the vacuum permeability, $M_s = |\boldsymbol{M}|$ is the saturation magnetization of the FL). For simplicity, we neglect any in-plane anisotropy of the FL.

The dynamics of the unit magnetization vector $\boldsymbol{m}(t) = \boldsymbol{M}(t)/M_s$ in the FL under the action of a microwave current $I_{\mathrm{RF}}(t) = I_{\mathrm{RF}} \sin(\omega t)$ is governed by the Landau-Lifshits-Gilbert-Slonczewski (LLGS) equation:

$$\frac{d\boldsymbol{m}}{dt} = \gamma \left[\boldsymbol{B}_{\mathrm{eff}} \times \boldsymbol{m}\right] + \alpha \left[\boldsymbol{m} \times \frac{d\boldsymbol{m}}{dt}\right]$$
$$+ \sigma I_{\mathrm{RF}}(t) \left[\boldsymbol{m} \times [\boldsymbol{m} \times \boldsymbol{p}]\right] , \quad (1)$$

where $\gamma \approx 2\pi \cdot 28$ GHz/T is the modulus of the gyromagnetic ratio, $\boldsymbol{B}_{\mathrm{eff}} = (B_0 - \mu_0 M_z)\hat{\boldsymbol{z}}$ is the effective magnetic field, M_z is the z-component of vector $\boldsymbol{M}$, α is the Gilbert damping constant, $\sigma = \sigma_\perp/(1 + P^2 \cos\beta)$ is the current-torque proportionality coefficient, $\sigma_\perp = (\gamma\hbar/2e)P/(M_s V)$, $\hbar$ is the reduced Planck constant, e is the modulus of the electron charge, P is the spin-polarization of current, β is the angle between the directions of magnetization in the FL and the PL ($\cos\beta = \boldsymbol{m} \cdot \boldsymbol{p}$), $V = \pi r^2 d$ is the volume of the FL (r is its radius and d is its thickness), and $\boldsymbol{p} = \hat{\boldsymbol{x}}$ is the unit vector in the direction of magnetization of the PL.

The angular dependence of the MTJ magnetoresitance can be written as

$$R(\beta) = \frac{R_\perp}{1 + P^2 \cos\beta} , \quad (2)$$

where $R_\perp$ is the junction resistance in the perpendicular magnetic state ($\beta = \pi/2$). The output DC voltage of the STMD is equal to

$$U_{\mathrm{DC}} = \langle I_{\mathrm{RF}}(t) R(\beta(t)) \rangle , \quad (3)$$

where the angular brackets denote averaging over the period $2\pi/\omega$ of the microwave current.

Equations (1)-(3) will be used below in analytical and numerical calculations of the STMD performance in the OOP-regime.

B. Analytical description of the OOP-regime

Using the spherical coordinate system for the magnetization vector $\boldsymbol{m} = \hat{\boldsymbol{x}} \sin\theta \cos\phi + \hat{\boldsymbol{y}} \sin\theta \sin\phi + \hat{\boldsymbol{z}} \cos\theta$, one can obtain the equations for the polar θ and azimuthal ϕ angles:

$$\frac{d\theta}{dt} = -\alpha\omega_P \sin\theta - \sigma I_{\mathrm{RF}} \sin(\omega t) \cos\theta \cos\phi , \quad (4a)$$
$$\frac{d\phi}{dt} = \omega_P + \sigma I_{\mathrm{RF}} \sin(\omega t) \csc\theta \sin\phi . \quad (4b)$$

Here $\omega_P \equiv \omega_P(\theta) = \omega_H - \omega_M \cos\theta$ is the frequency of magnetization precession in the OOP-regime, $\omega_H = \gamma B_0$, $\omega_M = \gamma\mu_0 M_s$. For simplicity, we neglected in Eqs. (4) second-order non-conservative terms ($\propto \alpha^2$ and $\propto \alpha I_{\mathrm{RF}}$), which have a negligible effect on the magnetization dynamics.

In the OOP precessional regime, the magnetization precesses around $\hat{\boldsymbol{z}}$ axis along approximately circular orbit, $\theta \approx$ const, $\phi \approx \omega t + \psi$, where ψ is the phase shift between the magnetization precession and the driving current. To analyze the conditions, under which the OOP regime is possible, one can average Eqs. (4) over the period of precession $2\pi/\omega$ and obtain the following equations for the slow variables θ and ψ:

$$\left\langle \frac{d\theta}{dt} \right\rangle = -\alpha\omega_P \sin\theta + v(a) \frac{\sigma_\perp I_{\mathrm{RF}}}{2} \cos\theta \sin\psi , \quad (5a)$$
$$\left\langle \frac{d\psi}{dt} \right\rangle = \omega_P - \omega + u(a) \frac{\sigma_\perp I_{\mathrm{RF}}}{2} \frac{1}{\sin\theta} \cos\psi . \quad (5b)$$

Here $a = P^2 \sin\theta$ and

$$v(a) = -\frac{2}{\sin\psi} \left\langle \frac{\sin(\omega t) \cos\phi}{1 + P^2 \sin\theta \cos\phi} \right\rangle \quad (6a)$$
$$= \frac{1}{\sqrt{1-a^2}} \left[1 + \left(\frac{\sqrt{1-a^2}-1}{a} \right)^2 \right]$$

$$u(a) = \frac{2}{\cos\psi} \left\langle \frac{\sin(\omega t) \sin\phi}{1 + P^2 \sin\theta \cos\phi} \right\rangle \quad (6b)$$
$$= \frac{1}{\sqrt{1-a^2}} \left[1 - \left(\frac{\sqrt{1-a^2}-1}{a} \right)^2 \right] .$$

Note, that for typical spin-polarization values $P \lesssim 0.7$ both dimensionless functions $u(a)$ and $v(a)$ are very close to 1 for all angles θ.

The OOP regime of magnetization precession corresponds to a stationary solution of Eqs. (5) $\theta = \theta_s = \text{const}$, $\psi = \psi_s = \text{const}$. Solving Eqs. (5) in this case one can find the stationary value of the phase shift ψ_s:

$$\sin \psi_s = 2 \frac{\alpha}{v} \frac{\omega_P}{\sigma_\perp I_{\text{RF}}} \tan \theta_s , \qquad (7a)$$

$$\cos \psi_s = 2 \frac{1}{u} \frac{\omega - \omega_P}{\sigma_\perp I_{\text{RF}}} \sin \theta_s . \qquad (7b)$$

Eliminating ψ_s from the above equations, one obtains characteristic equation for θ_s:

$$(\omega - \omega_P)^2 \sin^2 \theta_s + \frac{\alpha^2 u^2}{v^2} \omega_P^2 \tan^2 \theta_s = \frac{u^2}{4} \sigma_\perp^2 I_{\text{RF}}^2 . \quad (8)$$

This equation for θ_s is a nonlinear equation, which, in a general case, can be only solved numerically.

One can see that Eq. (8) has solutions only for RF currents I_{RF} larger than a certain critical current I_{th}. At the threshold, $\omega_P(\theta_s) \approx \omega$, which allows one to obtain approximate expression for the threhold precession angle

$$\theta_{\text{th}} \approx \frac{\pi}{2} - \frac{\omega_H - \omega}{\omega_M} \qquad (9)$$

and determine the threshold microwave current $I_{\text{th}}(\omega)$ needed for the excitation of the OOP precession:

$$I_{\text{th}}(\omega) = 2 \frac{\alpha}{v} \frac{\omega_M}{\sigma_\perp} \frac{\omega}{\omega_H - \omega} . \qquad (10)$$

In the last expression we used the approximation $\sin(\theta_{\text{th}}) \approx 1$, which is valid for moderate magnetic fields and frequencies $\omega_H, \omega \ll \omega_M$.

In order to analyze the stability of the magnetization precession in the OOP-regime we consider small deviations $\delta\theta$, $\delta\psi$ of variables θ, ψ near their stationary values θ_s, ψ_s, respectively. Specifically, one can substitute $\theta = \theta_s + \delta\theta$ and $\psi = \psi_s + \delta\psi$ in Eqs. (5), expand the equations in Taylor series and keep in the newly obtained equations only the terms that are linearly dependent on $\delta\theta$, $\delta\psi$. Taking into account that $\langle d\theta_s/dt \rangle = \langle d\psi_s/dt \rangle = 0$, one can obtain that the magnetization precession in the OOP-regime will be stable if the following approximate conditions are fulfilled:

$$0 < \cos \theta_s < \frac{\omega_H}{\omega_M} , \qquad (11a)$$

$$\omega < \omega_H . \qquad (11b)$$

The first condition given by Eq. (11a) means that the precession angle θ_s must be sufficiently large, because $\omega_H \ll \omega_M$ (we consider the case of a weak DC magnetic field) and $\cos\theta_s \ll 1$. The condition Eq. (11b) restricts the region of existence of the OOP-regime to sufficiently low driving frequencies, determined by the bias magnetic field B_0.

The output STMD voltage in the OOP-regime can be found using Eqs. (2) and (3) and noting that $\cos(\beta(t)) = \sin\theta_s \cos\phi(t)$:

$$U_{\text{DC}} = \langle I_{\text{RF}} R(\beta) \sin(\omega t) \rangle = w(a) I_{\text{RF}} R_\perp \sin \psi_s , \quad (12)$$

where

$$w(a) = \frac{1}{\sin\psi} \left\langle \frac{\sin(\omega t)}{1 + P^2 \sin\theta \cos\phi} \right\rangle \qquad (13)$$

$$= \frac{1}{\sqrt{1-a^2}} \left(\frac{1 - \sqrt{1-a^2}}{a} \right) .$$

Using Eq. (7a) for $\sin\psi_s$ allows one to get the DC voltage as a function of θ_s only:

$$U_{\text{DC}} = 2\alpha \frac{w}{v} \frac{\omega_P}{\sigma_\perp} R_\perp \tan \theta_s . \qquad (14)$$

This equation for U_{DC} can be simplified further by using the approximation $\sin\theta_s \approx 1$, $\cos\theta_s \approx \cos\theta_{\text{th}} \approx (\omega_H - \omega)/\omega_M$, valid for not very large driving currents:

$$U_{\text{DC}} \approx 2\alpha \frac{w}{v} \frac{\omega_M}{\sigma_\perp} R_\perp \frac{\omega}{\omega_H - \omega} . \qquad (15)$$

Comparing Eq. (15) with Eq. (10) for threshold current $I_{\text{th}}(\omega)$, one can re-write the output DC voltage of the STMD as the function of threshold current $I_{\text{th}}(\omega)$:

$$U_{\text{DC}} \approx w I_{\text{th}}(\omega) R_\perp . \qquad (16)$$

It follows from Eqs. (15), (16) that the output DC voltage of the STMD practically does not depend on the amplitude of RF current, provided that it is larger than the threshold current I_{th}.

III. PERFORMANCE OF A STMD IN OOP-REGIME

A. Typical parameters of a STMD

Below we shall analyze an analytical solution for the STMD in the OOP-regime of operation, compare this solution with the results of numerical calculations and then also compare the performance of the STMD in IP- and OOP-regimes.

We shall consider the case of the STMD with the following typical parameters (see e.g.[9,10]): radius of the STMD FL $r = 50\,\text{nm}$, thickness of the STMD FL $d = 1\,\text{nm}$, spin-polarization efficiency of current $P = 0.7$, resistance of STMD in perpendicular magnetic state ($\beta = \pi/2$) $R_\perp = \text{RA}/(\pi r^2) = 1\,\text{k}\Omega$ (giving resistance-area product of MTJ RA $= 7.854\,\Omega\,\mu\text{m}^2$), Gilbert damping constant $\alpha = 0.01$, saturation magnetization of the FL $\mu_0 M_s = 800\,\text{mT}$.

We choose the magnitude of the external out-of-plane DC magnetic field as $B_0 = 200\,\text{mT}$ for the STMD in OOP-regime, which corresponds to the maximum OOP frequency $\omega_H = 2\pi \times 5.6\,\text{GHz}$.
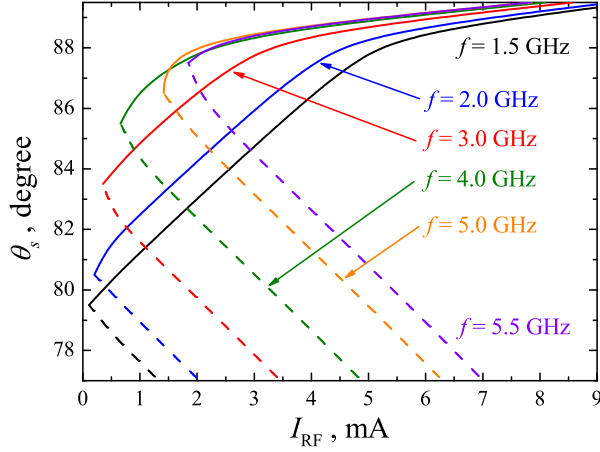
FIG. 2. The dependence of the OOP precession angle θ_s on the magnitude of RF current I_{RF} for different frequencies of RF signal $f = \omega/2\pi$ for an STMD with typical parameters (see Sec. III A). Solid lines correspond to the stable OOP-precession modes, while dashed lines correspond to the unstable trajectories. The minimum value of I_{RF} for any particular curve is the $I_{th}(\omega)$ of the OOP-precession mode.

In the IP-regime of operation, the STMD will be characterized by the equilibrium angle $\beta_0 = \pi/2$ between the equilibrium magnetization of the FL and the magnetization of the PL. Hence the equilibrium resistance of the STMD in the IP-regime is $R_0 = R_\perp = 1\,\mathrm{k\Omega}$. We choose the magnitude of the external DC in-plane magnetic field as $B_0 = 14.1\,\mathrm{mT}$ for the STMD in IP-regime, that in accordance with the expression for FMR frequency $f_0 = \omega_0/2\pi = (\gamma/2\pi)\sqrt{B_0(B_0 + \mu_0 M_s)}$ gives $f_0 = 3\,\mathrm{GHz}$. The resonance STMD sensitivity in the passive regime for such parameters is $\varepsilon_{res} \approx 2700\,\mathrm{V/W}$ (see e.g.[9]), which is greater or comparable to the sensitivity of a typical unbiased Schottky diode[10].

B. Precession angle and threshold current in the OOP-regime

Numerical solutions of Eq. (8) for the OOP precession angle θ_s as a function of the microwave current I_{RF} for several driving frequencies $f = \omega/2\pi$ are shown in Fig. 2. As one can see, the stable OOP-precession mode exists only for trajectories of magnetization motion with sufficiently large precession angles θ_s (see Eq. (11a)). With the increase of the driving current I_{RF} the precession angle θ_s monotonically increases up to the maximum value $\theta = \pi/2$.

Fig. 2 can also be used for the determination of the threshold current $I_{th}(\omega)$ needed for excitation of the OOP-precession regime. One can see that with the increase of the microwave frequency ω the threshold current $I_{th}(\omega)$ also increases. Our calculations show that the difference of $I_{th}(\omega)$ calculated from Eq. (8) and from approximate Eq. (10) is about several percent and, there-

fore, one can use analytical Eq. (10) for rather accurate estimation of the threshold current.

C. Performance of an STMD in the IP and OOP regimes

The precession motion of magnetization in the IP-regime determines the following typical properties of a traditional STMD[8–10]:

(a) The STMD operates as a frequency-selective microwave detector with a resonance frequency that is close to the frequency of ferromagnetic resonance (FMR) ω_0 of the FL;

(b) The frequency operation range of the detector has an order of the FMR linewidth Γ;

(c) The output DC voltage U_{DC} of the STMD is proportional to the input microwave power $P_{RF} = I_{RF}^2 R_0/2$ (R_0 is the equilibrium MTJ resistance), so the spin-torque diode operates as a resonance-type quadratic microwave detector:

$$U_{DC} = \varepsilon_{res} P_{RF} \frac{\Gamma^2}{\Gamma^2 + (\omega - \omega_0)^2} \ , \qquad (17)$$

where ε_{res} is the resonance (at $\omega = \omega_0$) diode volt-watt sensitivity (see[9]);

(d) the diode resonance sensitivity ε_{res} strongly depends on the angle β between magnetization directions of the FL and PL. The resonance sensitivity of traditional STMD $\varepsilon_{res} = U_{DC}/P_{RF}$ is predicted to be about $\varepsilon_{res} \sim 10^4\,\mathrm{V/W}$ (see[9]), while the best achieved to date experimental result is $\varepsilon_{res} \approx 300\,\mathrm{V/W}$[10].

We shall use the Eq. (17) for the calculation of the output DC voltage of an STMD in the IP-regime as a function of the input microwave current I_{RF} and current frequency ω. These curves are indicated below in Figs. 4 and 3 by red dashed lines.

In order to verify the conclusions of the analytical theory of an STMD in the OOP-regime we solved numerically the LLGS Eq. (1) and then numerically calculated the output DC voltage of the detector as $U_{DC} = \langle I_{RF}(t)R(\beta) \rangle$. The results of our calculations are presented in Figs. 3, 4. Here solid blue lines and red dashed lines present the analytical dependencies of U_{DC} in the OOP- and IP-regimes (see Eq. (16) and Eq. (17)), respectively. Dots are the results of our numerical calculations. Black crosses and green circles correspond to the cases of increasing and decreasing of the parameter (frequency ω or magnitude I_{RF} of the RF current), respectively. As one can see, the results of analytical theory are in reasonable agreement with the results of our numerical calculations.

As one can see from Fig. 3, in the OOP-regime the STMD works as a broadband low-frequency non-resonant microwave detector in contrast to the traditional resonance IP-regime. The response of the STMD to an input microwave current with magnitude I_{RF} is also substantially different in the cases of OOP- and IP-regimes of
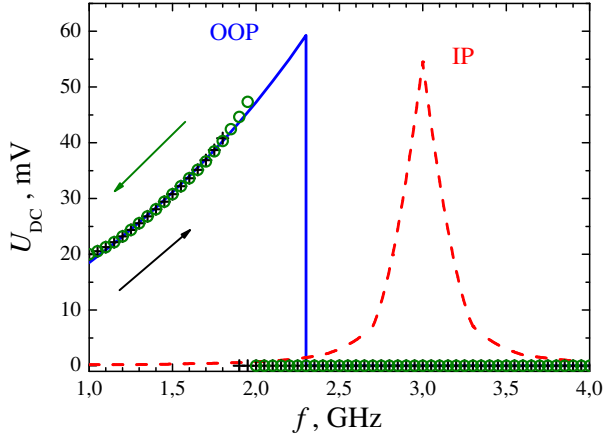
FIG. 3. The dependence of the output DC voltage U_{DC} of a STMD on frequency of input RF signal $f = \omega/2\pi$ in OOP- (solid line and points) and IP-regime (dashed line), respectively. Blue solid line is the analytical dependence given by Eq. (16), red dashed line is the analytical dependence given by Eq. (17). Points are the results of numerical simulations. Black crosses and green circles corresponded to the case when frequency is increased and decreased, respectively. $I_{\mathrm{RF}} = 0.2\,\mathrm{mA}$, all other parameters are the same as indicated in Sec. III A.
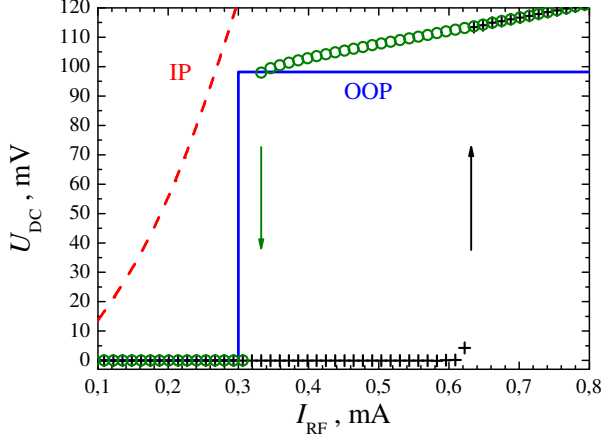

FIG. 4. The dependence of the output DC voltage U_{DC} of a STMD on input microwave current I_{RF} in OOP- (solid line and points) and IP-regime (dashed line), respectively. Blue solid line is the analytical dependence given by Eq. (16), red dashed line is the analytical dependence given by Eq. (17). Points are the results of numerical simulations. Black crosses and green circles corresponded to the case when the current is increased and decreased, respectively. $f = \omega/2\pi = 3\,\mathrm{GHz}$, all other parameters are the same as indicated in Sec. III A.

operation of an STMD (see Fig. 4). In the IP-regime, the output DC voltage U_{DC} of the detector is proportional to the input microwave power $P_{\mathrm{RF}} = (1/2)I_{\mathrm{RF}}^2 R_0$ (red dashed curve in Fig. 4, see also Eq. (17)). In contrast, the output DC voltage U_{DC} of the detector in the OOP-regime has a step-like dependence (blue solid curve and points in Fig. 4): $U_{\mathrm{DC}} \approx 0$ for $I_{\mathrm{RF}} < I_{\mathrm{th}}(\omega)$ and

$U_{\mathrm{DC}} \approx \mathrm{const}$ for $I_{\mathrm{RF}} > I_{\mathrm{th}}(\omega)$. Thus, in the OOP-regime, the STMD operates as a non-resonant broadband threshold microwave detector of low frequency RF signals.

It is important to note, that the results of our numerical simulations showed the existence of a hysteresis in the curves $U_{\mathrm{DC}}(f)$ and $U_{\mathrm{DC}}(I_{\mathrm{RF}})$ in the OOP-regime (see Figs. 3, 4). The origin of this hysteresis lies in the "hard", or subcritical, scenario of excitation of the OOP precession: the precession angle θ_{th} that corresponds to the threshold current I_{th} (see Fig. 2) does not coincide with the equilibrium magnetization angle and, therefore, for currents close to the threshold one the OOP regime may or may not be realized, depending on the history of the system. In experiments, the hysteresis may be "blurred" or may not be visible at all due to the influence of thermal fluctuations and other noises existing in real systems.

The results presented above correspond to the case of no DC bias current applied to the MTJ ($I_{\mathrm{DC}} = 0$). If this is not the case and $I_{\mathrm{DC}} \neq 0$, this current will partly compensate the damping in the FL MTJ, thus decreasing the threshold current $I_{\mathrm{th}}(\omega)$. On the other hand, the in-plane anisotropy and/or the in-plane bias field in the FL may create an energy barrier between the regions of small-angle IP- and large-angle OOP-trajectories, which may result in increase of I_{RF}.

We also suggest that the OOP-regime of operation of a STMD might be responsible for an extremely large diode volt-watt sensitivity $\varepsilon \sim 10^5\,\mathrm{V/W}$ observed in recent experiments with thermally-activated "non-adiabatic stochastic resonance"[11,12].

D. Energy harvesting applications of an STMD in OOP-regime

The STMD in the OOP-regime could be used as a base element for new energy harvesting devices, inasmuch as it has no resonance frequency, and, therefore, could accumulate energy from all the low-frequency region ($\omega < \omega_H$) of the microwave spectrum.

The energy conversion rate ζ of an STMD in the OOP-regime may be estimated as

$$\zeta = \frac{P_{\mathrm{DC}}}{P_{\mathrm{RF}}} \approx \frac{1}{2}\left(\frac{I_{\mathrm{th}}(\omega)}{I_{\mathrm{RF}}}\right)^2\left(\frac{w}{w_0}\right)^2, \qquad (18)$$

where P_{DC} is the output DC power of an STMD under the action of input microwave power P_{RF}, $w_0 \equiv w_0(a_s) = (1 - a_s^2)^{-1/2}$, $a_s \approx P^2$. The maximum possible conversion rate $\zeta_{\mathrm{max}} \approx 0.5 w^2/w_0^2 \approx 3.5\,\%$ is reached in the case $I_{\mathrm{RF}} = I_{\mathrm{th}}(\omega)$. We believe that his ratio is sufficiently large for practical applications in microwave energy harvesting.

IV. SUMMARY

In conclusion, it has been demonstrated that there is a novel regime of operation of an STMD, based on the excitation of large-angle out-of-plane (OOP) magnetization precession. In this regime STMD has the following features:

(a) it operates as a *non-resonant* broadband microwave detector for input RF currents I_{RF} larger than the critical current I_{th}, $I_{\mathrm{RF}} > I_{\mathrm{th}}$. Thus, STMD operates as *threshold* detector of RF signals;

(b) a stable OOP-regime exists for low frequency input signals with frequencies $\omega < \omega_H$;

(c) the output DC voltage U_{DC} in the OOP-regime has a step-like form and weakly depends on the magnitude of input RF current I_{RF} for currents $I_{\mathrm{RF}} > I_{\mathrm{th}}$.

We believe that the OOP regime of STMD operation can be used for the development of novel types of threshold microwave detectors and might be responsible for extremely large diode volt-watt sensitivity observed in recent experiments with "non-adiabatic stochastic resonance"[11,12]. This regime of operation of an STMD might also be useful for the creation of energy harvesting devices based on STMD, which operate in the low-frequency region of the microwave spectrum.

* Oleksandr.Prokopenko@gmail.com
[1] L. Berger, Phys. Rev. B **54**, 9353 (1996).
[2] J.C. Slonczewski, J. Magn. Magn. Mat. **159**, L1 (1996).
[3] G. Bertotti, C. Serpico, I.D. Mayergoyz, R. Bonin, and M. dAquino, Current-induced magnetization dynamics in nanomagnets, J. Magn.Magn. Mater.,**316**, 285 (2007).
[4] D.C. Ralph and M.D. Stiles, J. Magn. Magn. Mater., **320**,1190(2008).
[5] D.V. Berkov and J. Miltat, J. Magn. Magn. Mater.,**320**,1238(2008).
[6] T.J. Silva and W.H. Rippard, J. Magn. Magn. Mater., **320**,1260(2008).
[7] A. Slavin and V. Tiberkevich, IEEE Trans. Magn. **45**, 1875 (2009).
[8] A.A. Tulapurkar, Y. Suzuki, A. Fukushima *et al.*, Nature (London) **438**, 339 (2005).
[9] C. Wang, Y.-T. Cui, J.Z. Sun *et al.*, J. Appl. Phys. **106**, 053905 (2009).
[10] S. Ishibashi, T. Seki, T. Nozaki *et al.*, Appl. Phys. Express **3**, 073001 (2010).
[11] X. Cheng, C.T. Boone, J. Zhu, and I.N. Krivorotov, Phys. Rev. Lett. **105**, 047202 (2010).
[12] X. Cheng, C.T. Boone, J. Zhu, and I.N. Krivorotov, Abstracts of the 55th Annual Conference on Magnetism and Magnetic Materials (MMM 2010), EC-03, Atlanta, Georgia, November 2010.